Infrared and Fluorescence Properties of Reduced Graphene Oxide/Regenerated Cellulose Composite Fibers

Xue Wang, Qinglin Yan, Xin Gao, Shuangxin Wang, Yuyu He, and Liping Zhang *

To give cellulose fibers dual characteristics of warming and fluorescence, graphene oxide (GO) and fluorescent particles were simultaneously dispersed into the regenerated cellulose spinning solution through blending modification and post-reduction methods. After dry-jet wet spinning and reducing in hydrazine hydrate solution, the reduced graphene oxide (RGO)/regenerated composite fibers with different mass ratios of filler were completed. Fourier-transform infrared spectroscopy (FTIR), X-ray diffraction (XRD), scanning electron microscopy (SEM), fluorescence microscopy, and other methods were used to characterize the structure and morphology of fibers. Test results showed that the thermal stability and infrared emissivity increased gradually with the increase of GO. The crystallinity and strength of the composite fiber first increased and then decreased. This type of fiber also had luminescent properties after addition of fluorescent agent. However, when too much fluorescent agent was added, the thermal stability, infrared emissivity, crystallinity, and other properties mentioned above were affected to some extent. According to the comprehensive analysis, when the amount of GO added was 1 wt% and fluorescent added was 3 wt%, respectively, the luminescence characteristic and far-infrared emissivity of the fibers were remarkably improved.

Keywords: Reduced graphene oxide; Regenerated cellulose; Infrared emissivity, Fluorescence properties

Contact information: MOE Engineering Research Center of Forestry Biomass Materials and Bioenergy, Beijing Forestry University, Beijing 100083, *China; *Corresponding author: zhanglp418@163.com*

INTRODUCTION

A major current focus on green energy revolution has forced researchers to develop renewable, degradable, and environmentally friendly fiber materials. Regenerated cellulose fiber, which is regenerated from natural cellulose, due to its environmental protection properties and easy availability, has become an ideal material that can substitute for conventional synthetic fiber (Liu *et al.* 2019). It has a wide range of sources, but due to the shortage of forestry resources, straw resources are now being considered as alternative cellulose sources where the cellulose content can reach up to 30 to 50%. However, at present, straw has not been used effectively, except for a small part of papermaking, energy, *etc.* (Kim *et al.* 2006). Most of the straw is burned, which pollutes the environment and causes waste of resources (Liang *et al.* 2018). Therefore, isolating cellulose from agricultural waste to prepare regenerated cellulose fiber is one of the ways to utilize straw resources in high value. Composite fiber possesses some outstanding and comparable properties, and extends its applications for special materials (Saba *et al.* 2016). In recent years, fibers with functions, such as thermal insulation and fluorescence, have aroused great interest. They can be used not only in the field of textiles, but also in transportation,

anti-counterfeiting, and in other fields. Thus, functional compounding is an important way to increase the value of cellulose fibers.

Graphene has attracted a lot of attention in recent years, especially in the area of composite materials. Since the first graphene fiber was obtained by Gao's research group of Zhejiang University in 2011, various structures and compositions of graphene fibers have been investigated, broadening the field of view for the research of excellent performing composite fibers (Zhang and Chen 2019). The unique two-dimensional sheet structure (Allen *et al.* 2010) and large specific area of graphene account for their remarkable mechanical and thermal properties (Mahmoudian *et al.* 2017). In particular, graphene is both a far-infrared absorber and a good radiator. It has a far-infrared energy storage function (Tang *et al.* 2014), which can produce a series of physiological responses to the human body, increasing microcirculation and metabolism. Moreover, chemically modified graphene sheets also possess these characteristics (Zhang *et al.* 2010), which makes it possible to produce warm fibers. To address such a property, several efforts have been applied through blending spinning and coating methods. The development of the latter method was restricted by its poor uniformity and stiff feeling (Du *et al.* 2016). In contrast, the former method is permanent and currently widely used in the research of synthetic fibers and viscose fibers. In this study the authors used chemical reduction and post-treatment methods to prepare reduced graphene oxide (RGO) regenerated cellulose fiber. The diluted oxygen-containing functional groups of RGO can benefit the combination with cellulose (Sawangphruk *et al.* 2013), it is also a simple way to realize batch production.

In addition to the far infrared properties, fluorescent fiber is another functional fiber that attracts much attention. Many attempts have been focused on the fluorescent fiber materials in recent years. Under the specific wavelength of excitation light, the fluorescent fiber can radiate fluorescence, thereby displaying the target in the dark. The fluorescent characteristic not only plays an increasingly important role in the fields of stage performance, but transportation, firefighting, and security fields (Zhang *et al.* 2016). To date, blending modification is mainly an approach to make fluorescent fiber, including melt spinning, solution spinning, electrospinning, *etc*. Among them, solution spinning possesses broad prospects (Zhao *et al.* 2012) because of its low temperature, convenient operation, and it does not cause the problem of thermal decomposition. In 1936, the French scientist Georges Destriau discovered that an inorganic adjunct, such as zinc sulfide, can exhibit an electroluminescent effect. Compared with organic fluorescent substances, inorganic salt fluorescent materials have the characteristics of heat resistance, good solubility, and strong stability (Wang 2015). Through mechanical blending modification and coupling with the cross-linking agent at the same time, the fluorescent substance can be added to the cellulose matrix (Liao *et al.* 2018).

In this study, the authors complexed different agents to a cellulose matrix, aiming to prepare the multifunctional textiles used in thermal or optical equipment. Straw pulp, which was dissolved in a novel ionic liquid to prepare a spinning solution, was selected as the raw material. After incorporating graphene oxide (GO) and Zns:Cu fluorescent agent into the spinning solution, the chemical reduction treatment was employed after dry-jet wet spinning to achieve reduced graphene oxide/regenerated cellulose composite fibers. The effects of additives on the chemical structure, crystallinity, surface morphology, and thermal stability of fibers were discussed using Fourier transform infrared (FTIR), X-ray diffraction (XRD), scanning electron microscopy (SEM), thermogravimetric analysis (TGA), and other analyses. Moreover, the fluorescence spectroscopy, fluorescence

microscopy, and far-infrared emissivity were also used to test the corresponding properties of the composite fiber.

EXPERIMENTAL

Materials

Straw pulp, within which the content of cellulose was more than 90 wt%, was obtained from Jilin Chemical Fiber Group Co., Ltd. (Jilin Province, China). The novel ionic liquid was made by the authors. The graphene oxide was purchased from Leadernano Tech LLC (Shandong Province, China). The hydrazine hydrate (> 98% (Technical grade)) was supplied by Shanghai Aladdin Bio-Chem Technology Co., Ltd. (Shanghai, China). The ethanol absolute, ZnS:Cu fluorescent (micron size) and Titanate coupler (cp) were supplied by Beijing Chemical Works (Beijing, China).

Methods

The composite fibers were prepared used three main processes as follows:

(1) Pretreatment of fluorescent

A total of 10 wt% of ZnS:Cu powder and 8.34 wt% of titanate coupler were added to predetermined ethanol and mechanically stirred at room temperature for 1 h to make them uniformly mixed. After that, evaporation was completed under vacuum at 100 ℃ to remove the ethanol.

(2) Preparation of RGO/regenerated cellulose fibers

The straw pulp was dissolved in ionic liquid, different amounts of graphene oxide powder was added and uniformly dispersed in the cellulose spinning solution by mechanical stirring. This solution then was transferred to glass syringes for deaeration (still) at room temperature. The method of dry-jet wet spinning was used in this study. The fiber from spinneret would first via a dry air region and then stepped into coagulation bath, thus achieved double diffusion of solvent as well as high degrees of jet-stretch ratios. After that, the GO/regenerated cellulose fibers were prepared. To obtain RGO/regenerated cellulose fiber, the above fibers were reduced by hydrazine hydrate for at least 24 h and finally dried at room temperature.

(3) Preparation of RGO/regenerated cellulose fluorescent fibers

Table 1. Fiber Samples with Different Additive Ratios

Name	Cellulose Concentration of Spinning Solution (wt%)	GO Addition Amount (wt%)	Fluorescent Addition Amount (wt%)
Z-0	4	0	0
Z-0.5		0.5	0
Z-1		1	0
Z-2		2	0
Z-3		3	0
H-1		1	1
H-3(G-1)		1	3
H-5		1	5
G-0.5		0.5	3
G-2		2	3

The pretreated fluorescent agents obtained in (1) were further added in the graphene oxide regenerated cellulose spinning solution prepared in (2), the mixture was mechanically stirred for 2 h to mix uniformly. The above-mentioned spinning solution was transferred to a glass syringe and the subsequent procedures were same as (2). The addition ratio of GO and fluorescent in different fibers are shown in Table 1.

Characterization

The chemical fiber structure was analyzed using a German Bruker VERTES TOV FTIR instrument (Tensor 27; Bruker, Karlsruhe, Germany). The scanning range was from 500 to 4000 cm^{-1}. Fiber surface images were taken with SEM (Hitachi S-3400N II; Hitachi, Tokyo, Japan) after being coated with a thin layer of gold. The TGA under nitrogen was performed with a STA449F3 thermogravimetric analyzer (NETZSCH, Bavaria, Germany) to obtain a thermal decomposition curve. The temperature rise range was from room temperature to 450 ℃ with the rate of 20 ℃/min. The X-ray patterns of fluorescers and fiber powder were analyzed in a reflection mode on an X-ray diffractometer (D8 ADVANCE; Bruker, Karlsruhe, Germany). The samples were tested with Cu Ka radiation (k = 0.154 nm) at 40 kV and 30 mA with a scan speed of 2°/min from 5° to 50°. For the fluorescence properties of the fiber, the following two characterization methods were applied. Fluorescence spectroscopy was performed using a transient/steady-state fluorescence spectrometer (FLS920; Edinburgh Instruments, Bath, England). The fluorescence fiber powder was analyzed using only the stable test portion of the instrument. After the sample was stimulated at a wavelength of 365 nm, the fluorescence emission spectrum was obtained in the range of 400 to 700 nm. To observe the distribution of the luminescent particles on the fibers, the American fluorescent universal microscope BX61 (Olympus, Tokyo, Japan) was also used under the 100-fold bright field, which would help to tell the overall fluorescence performance of the fibers. The mechanical properties of the fibers were tested using a Zwick Roell 2.5Z stretcher (Instron, Canton, NJ, USA), whose distance between the clamps was 5 cm and tensile speed was fixed at 0.2 mm/s room temperature. Each sample was tested 10 times for averaging. In the end, for the convenient detection of infrared emissivity, the spinning solution was formed into films and then solidified in a hydrazine hydrate solution for 24 h. The film thickness was consistent. The IR-2 type dual-frequency infrared emission tester (Huaruison Co., Ltd., Beijing, China) was used with the wavelength of 8 to14 μm at 300 K to analyze the fiber films.

RESULTS AND DISCUSSIONS

FTIR Analysis

To verify the changes of chemical structure, FTIR spectroscopic analysis of Z-0, Z-1, and H-3 were performed, and the results are shown in Fig. 1. In the spectra of Z-0, a strong absorption band near 3400 cm^{-1}, characteristic of free O-H stretching vibration, was observed. The slight decrease at 3000 cm^{-1} was ascribed to C-H stretching vibration. Typical peaks of the C=C group at 1700 were exhibited. Meanwhile, water absorption also produces a certain degree of absorption (Li *et al.* 2015). The weak band in the spectral region of 1010 to 1100 cm^{-1} was assigned to the stretching vibration of C-O group (Alemdar and Sain 2008).

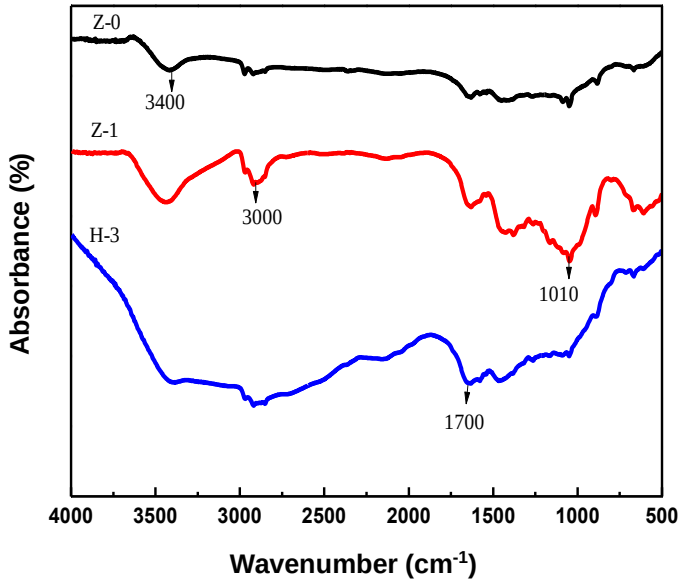

Fig. 1. FT-IR spectra of Z-0, Z-1, and H-3 fiber samples

Through comparison with Z-0, the broad and strong absorption peak around 3400 cm^{-1} was also exhibited in Z-1 and H-3. Moreover, the absorption peak became broad with the addition of RGO and fluorescent, which confirmed that the number of hydrogen bonds as well as intramolecular association hydrogen bonds in the system increased due to the addition agents (Lu 2014). The intensity of the C-H stretching vibration peak near 3000 cm^{-1} was higher than that in Z-0, which may have been related to the reduction of GO. The position of the band at 1700 cm^{-1} was accompanied with a slight shift compared with Z-0, the intensity here increased due to C=C bonds that not only presented in cellulose but in RGO powder. Especially in the spectra of Z-1, the absorption intensity at 1010 cm^{-1} was stronger than Z-0, which was attributed to the amount of oxygen-containing functional groups including C-O-C and -OH on the surface of the RGO (Li *et al.* 2017). In conclusion, the absorption peaks of Z-1 and H-3 fibers were similar to those of Z-0, indicating that the main groups present in the fiber samples prepared by the above method did not change.

Fiber Morphology

The SEM images of composite fibers and pure fibers are shown in Fig. 2. Cellulose fiber in Fig. 2a had an approximate cylindrical shape and smooth surface with no obvious ravines, which resulted from the absence of additives and the process of dry-jet wet spinning, thus making the formation uniform (Jiang *et al.* 2019). The composite fibers presented small particles and obvious ravines distributed unevenly on the surface. It was clear that the more substances added, resulted in a rougher surface. This was because GO and fluorescent particles destroyed the spinning fluency and the dense structure between macromolecules (Li *et al.* 2017), making grains on H-3 fiber more pronounced. In addition, the solvent that was not removed may also result in the protrusion parts of the fiber surface (Bazbouz *et al.* 2019). The ravines on the fibers may affect the intensity of fibers and make them more easily broken.

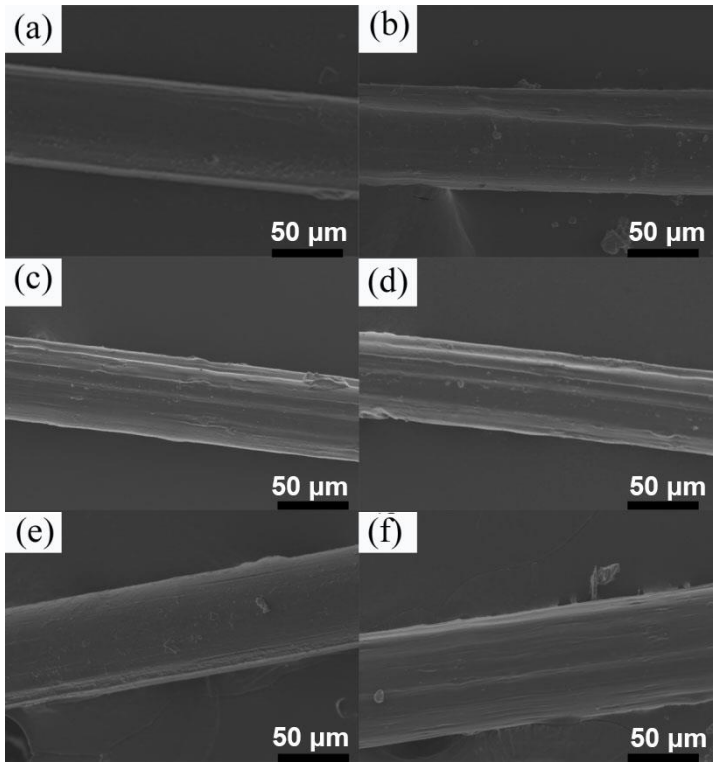

Fig. 2. SEM micrographs of fibers with different addition amounts: (a) Z-0, (b) Z-1, (c) Z-2, (d) Z-3, (e) H-1, and (f) H-3

TGA Analysis

The TGA and derivative thermogravimetric (DTG) curves of the sample are shown in Fig. 3A and 3B. The samples display approximately 70% mass loss from 100 to 400 ℃. The first mass loss at approximately 100 ℃ was due to the evaporation of H_2O and other chemicals (Yu *et al.* 2003). The subsequent weight loss in the range of 250 to 350 ℃ was the decomposition of cellulose fibers (Wang *et al.* 2015).

The temperature at maximum weight loss was delayed in Z-1 and H-3 compared with Z-0, the rate of loss of weight became decreased, and this trend was gradually upward with the increase of GO. Therefore, the regenerated cellulose fiber modified by RGO can significantly present better thermal stability (Greiner and Wendorff 2007). For composite fluorescent fiber (H-3), the range of degradation temperature was reduced compared to Z-1, which may have been related to the decrease in crystallinity of fiber after adding fluorescent.

XRD Analysis

The influence of RGO and fluorescent on crystallinity was examined by X-ray diffraction. The peaks of ZnS on JCPDS (Joint Committee on Powder Diffraction Standards) card were 28.58°, 33.12°, and 47.61°, corresponding to (111), (200), and (220) planes, respectively (Espinosa *et al.* 2019). Figure 4 shows the X-ray diffraction patterns of the fluorescent and fibers in this study. Compared to the study researched by Espinosa's group, the visible peaks were approximately at the same location, thus clarifying that this type of fluorescent is ZnS. The characteristic high peak and the sharp shape in the XRD patterns illustrate that the fluorescent atoms are arranged more regularly and a fine crystal structure is formed (Wang 2014).

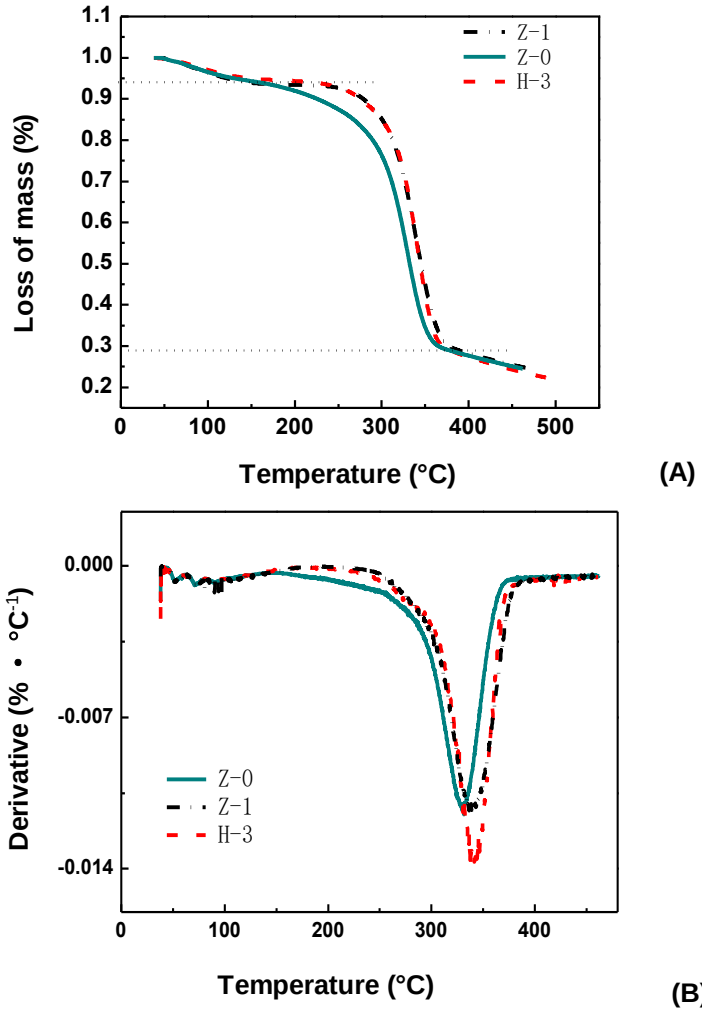

Fig. 3. A) TGA of Z-0, Z-1, and H-3 fiber sample; B) DTG of Z-0, Z-1, and H-3 fiber sample

From the XRD patterns of Z-0, Z-1, Z-3, and H-3, the authors found that the diffraction peaks of different fibers located at 12.19°, 20.18°, and 20.76° can be assigned to cellulose II (Zhang *et al.* 2018). This indicated the cellulose structure was converted from cellulose I to cellulose II after being regenerated, and the peaks became broad and weak due to the decrease of crystallinity. For the XRD of RGO reduced by hydrazine hydrate, a broad reflection peak centered at 24° is observed in the pattern researched by Zhang's group (Zhang *et al.* 2010). However, its characteristic peaks are not clearly shown in this pattern. This may have a certain degree of coincidence with the diffraction peak near 22.5° of cellulose II. In addition, the content of RGO in the solution is low and the diffraction intensity might be too weak to present (Li *et al.* 2019a). The crystallinity of Z-0, Z-1, and Z-3 were 35.9%, 40.2%, and 31.2%, respectively, confirming that the crystallinity can be improved with the addition of a certain amount of GO (Ouyang *et al.* 2013). However, the crystallinity decreased with the increase of the GO and fluorescent when the content of additives exceeded 1 wt%. This may have been because the particles gathered may have destroyed the hydrogen bond between the cellulose macromolecules, and thus the dense structure of the cellulose would be damaged.

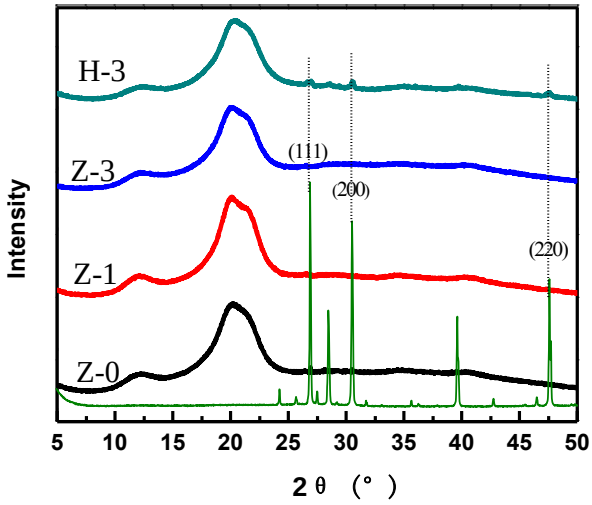

Fig. 4. X-ray diffraction pattern of fluoresce complex and Z-0, Z-1, Z-3, and H-3 fiber sample

H-3 exhibited new diffraction peaks at 26.99°and 34.84°, demonstrating that the fluorescent was successfully added to the composite fiber. Furthermore, Compared with Z-1 fiber, the crystallinity of H-3 sample decreased to 26.1%, which may have been influenced by the fluorescent and GO added during crystal growth, resulting in a decrease in crystallinity (Zhang *et al.* 2003). Therefore, when fluorescent is added to the fiber, it may prevent the action of RGO from increasing the crystallinity to some extent.

Fluorescence Spectra Analysis

Figure 5 is the fluorescence spectrum of H-1, H-3, and H-5 fibers. It has been studied that after excitation at a wavelength of 365 nm, S^{2-} in ZnS:Cu fluorescent can have an emission maxima at approximately 430 nm and a broad blue-green fluorescence emission peak at approximately 530 nm (Small and Johnston 2008).

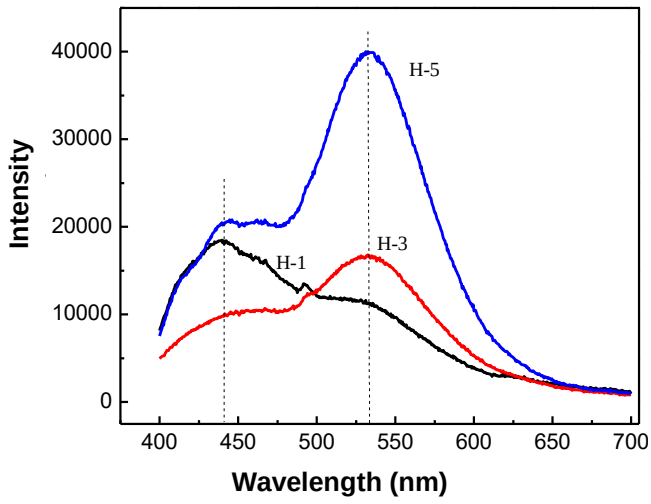

Fig. 5. Fluorescence spectra of fluorescence cellulose fiber with different concentrations

In the authors' research, all three curves had strong emissions at approximately 430 nm at different levels. H-3 and H-5 fibers also showed the highest intensity at approximately 530 nm, illustrating that the result was the same as the spectra measured in

the current study, verifying the fluorescent agent prepared in this study was ZnS:Cu fluorescent (Cui *et al.* 2018). It is worth noting that, in the location of 530 nm, the emission intensity tended to increase distinctly upon the increase of fluorescent, which suggests that the intensity at this wavelength was positively correlated with the concentration of fluorescent. However, the intensity had no obvious relationship at 430 nm with the amount of fluorescent, which may have been related to the dispersion degree of fluorescent and RGO. In general, the composite fibers had different degrees of fluorescence emission capability after addition of ZnS:Cu fluorescent.

Fluorescence Microscopy Characterization

Figure 6 shows the fluorescent microscope images before (a) and after (b) the treatment by coupling agent. The fluorescent powder showed obviously under blue light optical filter. Before treated with coupling agent, the fluorescent agent was finely granulated and densely dispersed in the field of view. Due to the inorganic characteristic, it was difficult for the fluorescent to uniformly disperse into the organic cellulose spinning solution, thus affecting the fluorescence properties of the fiber. Herein, after addition of coupling agent, most of the dispersed small particles became gathered. This was because low molecular mass chains that existed in the coupling agent reacted with the inorganic agents to form a molecular layer, thereby linking to the inorganic molecule. Other parts of the long chain intertwine with the cellulose polymer (Guo *et al.* 2003). In this way, the inorganic substance and the cellulose are tightly integrated by the 'media' coupling agent, so that the fluorescent can be uniformly dispersed in the cellulose spinning solution.

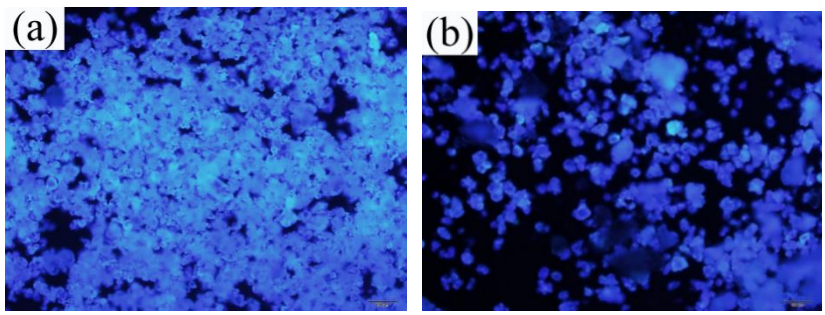

Fig. 6. Fluorescence microscopy characterization (a) before and (b) after pretreatment

Figure 7 shows the fluorescence microscope images of H-1, H-3, and H-5 cellulose fibers containing different fluorescent. It is well known that the larger aggregates are the main factors that influence the mechanical properties of fiber (Zhang *et al.* 2016). To pursue the dual characteristics of mechanical and fluorescent properties, one of the key methods is to prevent the agglomeration of fluorescent powder and improve the compatibility between fluorescent powder and the cellulose matrix. It can be seen from Fig. 7(a) that there were fewer fluorescent particles in the field of view, and the fluorescence characteristic was not obvious when the fluorescent was under 1 wt%. By contrast, in H-3 the 3 wt% addition of couple agent was dispersed homogeneously, as shown in Fig. 7(b), and the fluorescence characteristic was clearly observed. When fluorescent exceeded 5 wt%, the fiber was partially bright and the brightness was uneven; moreover, the self-agglomeration of the fluorescent is observed (Zhao *et al.* 2012). In summary, the composite fiber with 3 wt% fluorescent possessed better fluorescence characteristic.

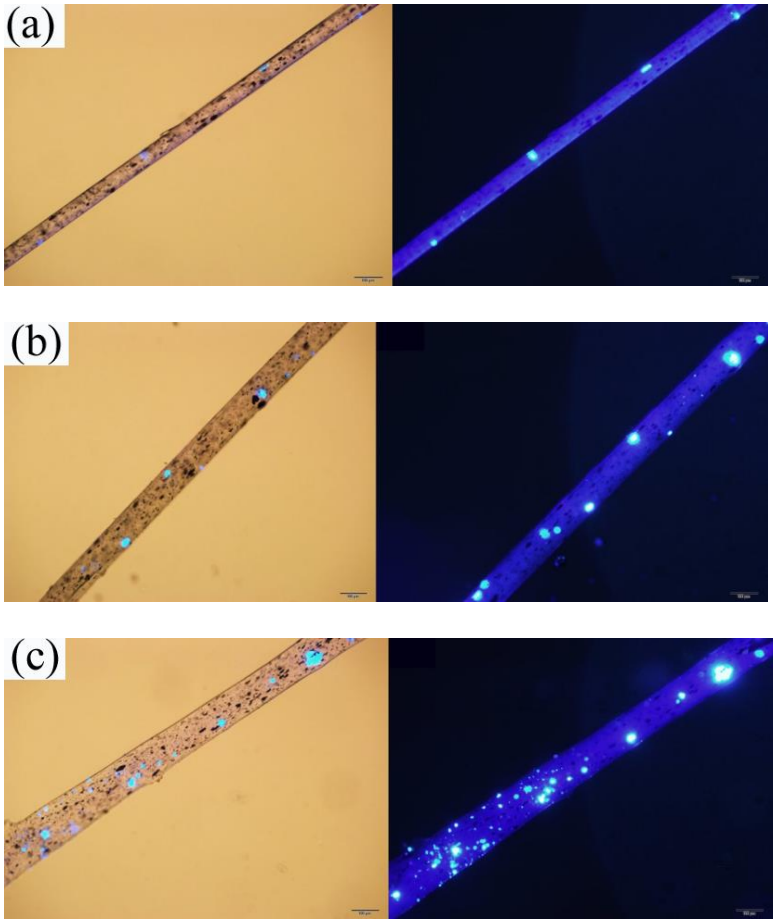

Fig. 7. Fluorescence microscopy characterization of composite fibers: (a) H-1, (b) H-3, and (c) H-5

Mechanical Properties

The mechanical properties of fibers at room temperature including tensile strength and elongation at break are listed in Table 2. As the proportion of RGO increased, the intensity of the composite fibers first increased and then decreased.

Table 2. Physical Material Property of Fibers with Different Addition Amount

Name	Intensity(cN/dtex) (1dtex = 1 g/10000 m)	Elongation at Break (%)
Z-0	2.230	14.4
Z-1	2.294	10.8
Z-2	2.282	10.0
G-0.5	1.941	5.08
H-3	2.030	6.40

When fibers were blended with 1 wt% GO, the material could withstand a stress as high as 2.294 cN/dtex, which was 3% higher than that of the pure regenerated cellulose fiber, indicating appropriate RGO will improve the strength of the fiber (Li *et al.* 2019b). The high fracture strain is attributed to the RGO with better performance as well as the good coherence between the regenerated cellulose matrix and RGO (Li *et al.* 2017). However, when content of GO exceeded 1 wt%, the degree of crystallinity was lowered

due to agglomeration between GO particles, resulting the decrease in intensity. Fluorescent particles have the same effect on fibers, so the dense crystal structure of the regenerated cellulose is further destroyed due to the self-aggregation of the fluorescer particles; thus the intensity of G and H groups was lower than that of the Z group. Compared to Z-1, H-3 had a reduction of approximately 13%. In addition, the tendency of elongation at break continued to decrease. Therefore, the addition of additives may cause local brittleness and reduce the toughness of fiber (Luzi *et al.* 2016).

Infrared Emissivity Analysis

Figure 8 shows the relationship between additives content and infrared emissivity of composite fibers. It shows noticeable enhancement of the emissivity value with respect to the bare cellulose fiber. Graphene, which has strong light absorption ability, can absorb light in all wavelength bands and output in the form of far infrared energy (Zhao *et al.* 2019). Many hydroxyl groups and C-H bonds on cellulose surface can form CH-π interaction with graphene, thus improving the performance of cellulose. So the far-infrared emissivity of the composite fiber membrane was obviously higher than that of the regenerated cellulose fiber membrane. When the content of GO increased, the value of far-infrared emissivity increased as well. When GO was 1 wt%, the far-infrared emissivity reached a maximum of 0.96. While the graphene content exceeded 1 wt%, the tendency was constant and even lower.

Concerned with the conclusion obtained in the fluorescence characterization above, to analyse the influence of fluorescent, 3 wt% ZnS:Cu fluorescent was further added to the above-mentioned fiber spinning solution to investigate the far-infrared emission properties of the fiber membrane, as also shown in Fig. 8.

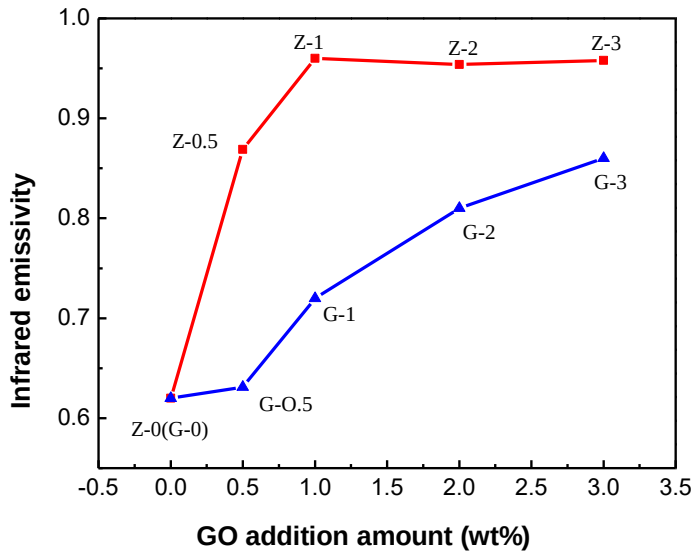

Fig. 8. The infrared emissivity of cellulose membrane

The emissivity showed an obvious reduction tendency compared with the line on the top, which indicates that the improvement on far-infrared emissivity by the function of RGO will be inhibited by fluorescent agent to some extent. However, compared to pure regenerated cellulose at 0.62, the emissivity will gradually increase to 0.72 when the content of GO reaches 1 wt%. The presence of GO took an essential effect on infrared

emissivity even if other agents were added to the matrix. The addition of the fluorescent will delay the maximum peak. According to mechanical analysis, if GO content continuously increased, the crystallinity of the fiber will be lowered to affect the properties such as intensity and elongation at break. In addition, the far-infrared emissivity of the film is also related to the surface condition such as roughness, color, and thickness of the film.

CONCLUSIONS

The regenerated cellulose fibers were modified by the combination of graphene oxide (GO) and fluorescent agent through post-reduction treatment, the effects of different contents of additives on the infrared emissivity and fluorescence characteristics were investigated.

1. To prepare reduced graphene oxide (RGO)/regenerated cellulose, GO was only added to the spinning solution. With the increase of GO addition, the mechanical strength, crystallinity, thermal stability, and infrared emissivity of the fiber were improved. When the addition amount was 1 wt%, the far-infrared emissivity of composite fiber reached the peak at 0.96. When the GO content was more than 1 wt%, the above properties of the fiber tended to decrease due to the agglomeration of addition particles.
2. If GO and fluorescent agent were added to spinning solution simultaneously, fibers containing 3 wt% of fluorescent agent had good luminescent properties, but the ZnS:Cu fluorescent agent hindered the improvement of thermal stability, crystallinity, mechanical properties, infrared emissivity, *etc.*, so that their performance values were slightly lower than single functional graphene fiber. In all, in the experimental range, when the fluorescent and GO content was 3 wt% and 1 wt%, respectively, the fiber emitted light uniformly, and the far-infrared emissivity increased 16% compared with the pure regenerated cellulose fiber. Other properties, such as crystallinity, were also greatly improved.
3. Through modification of the fibers by blending two additives into the cellulose matrix, the fibers can simultaneously obtain the characteristics of fluorescence and infrared emissivity, which makes it a possible way to prepare multi-functional fibers used in special clothing and sensors. On the basis of studying the influence of addition content, the additive size, choice of the dispersion system, and the modification method can also effect the performance of fibers.

REFERENCES CITED

Alemdar, A., and Sain, M. (2008). "Isolation and characterization of nanofibers from agricultural residues - Wheat straw and soy hulls," *Bioresource Technology* 99(6), 1664-1671. DOI: 10.1016/j.biortech.2007.04.029

Allen, M. J., Tung, V. C., and Kaner, R. B. (2010). "Honeycomb carbon: A review of graphene," *Chemical Reviews* 110(1), 132-145. DOI: 10.1021/cr900070d

Bazbouz, M. B., Taylor, M., Baker, D., Ries, M. E., and Goswami, P. (2019). "Dry-jet wet electrospinning of native cellulose microfibers with macroporous structures from

ionic liquids," *Journal of Applied Polymer Science* 136(10), Article number 47153. DOI: 10.1002/app.47153

Cui, T. T., Zhu, Z. J., Cheng, R., Tong, Y. L., Peng, G., Wang, C. F., and Chen, S. (2018). "Facile access to wearable device *via* microfluidic spinning of robust and aligned fluorescent microfibers," *ACS Applied Materials & Interfaces* 10(36), 30785-30793. DOI: 10.1021/acsami.8b11926

Du, M. Z., Tian, M. W., and Qu, L. J. (2016). "Research progress of far-infrared textiles and novel graphene far-infrared functional textiles," *Journal of Chengdu Textile College* 33(4), 132-137. DOI: 10.3969/j.issn.1008-5580.2016.04.028

Espinosa, E., Rol, F., Bras, J., and Rodriguez, A. (2019). "Production of lignocellulose nanofibers from wheat straw by different fibrillation methods. Comparison of its viability in cardboard recycling process," *Journal of Cleaner Production* 239, WOS:000487237100103. DOI: 10.1016/j.jclepro.2019.118083

Greiner, A., and Wendorff, J. H. (2007). "Electrospinning: A fascinating method for the preparation of ultrathin fibres," *Angewandte Chemie-International Edition* 46(30), 5670-5703. DOI: 10.1002/anie.200604646

Guo, Y. L., Zhang, S. R., and Li, L. P. (2003). "Types, characteristics and applications of coupling agents," *China Rubber Industry* 11, 692-696.

Jiang, Z. M., Tang, L., Gao, X., Zhang, W. T., Ma, J. W., and Zhang, L. P. (2019). "Solvent regulation approach for preparing cellulose-nanocrystal-reinforced regenerated cellulose fibers and their properties," *ACS Omega* 4(1), 2001-2008. DOI: 10.1021/acsomega.8b03601

Kim, M. S., Baek, J. S., Yun, Y. S., Sim, S. J., Park, S., and Kim, S. C. (2006). "Hydrogen production from *Chlamydomonas reinhardtii* biomass using a two-step conversion process: Anaerobic conversion and photosynthetic fermentation," *International Journal of Hydrogen Energy* 31(6), 812-816. DOI: 10.1016/j.ijhydene.2005.06.009

Li, C. L., Ma, J. Z., Qin, C. M., Qu, L. J., and Tian, M. W. (2015). "Preparation and properties study of graphene/regenerated cellulose composite fiber," *Knitting Industry* 6, 6-8.

Li, X. M., Zhang, K. K., Shi, R., Ma, X. M., Tan, L. W., Ji, Q., and Xia, Y. Z. (2017). "Enhanced flame-retardant properties of cellulose fibers by incorporation of acid-resistant magnesium-oxide microcapsules," *Carbohydrate Polymers* 176, 246-256. DOI: 10.1016/j.carbpol.2017.08.096

Li, N., Ma, Z. K., Chen, M., Song, H. H., Li, A., and Jia, Y. R. (2017). "Structures and performance of graphene/polyimide composite graphite fibers," *Journal of Materials Engineering* 45(9), 31-37. DOI: 10.11868/j.issn.1001-4381.2016.000251

Li, S., Chen, Z. F., Rao, Z. Y., Wang, F., Wu, C., and Ye, X. L. (2019a). "The preparation and research of reduced graphene oxide/glass composite fiber," *Journal of Engineered Fibers and Fabrics* 14, WOS:000495663600001. DOI: 10.1177/1558925019883105

Li, X., Li, H. C., You, T. T., Wu, Y. Y., Ramaswamy, S., and Xu, F. (2019b). "Fabrication of regenerated cellulose membranes with high tensile strength and antibacterial property *via* surface amination," *Industrial Crops and Products* 140, Article ID 111603. DOI: 10.1016/j.indcrop.2019.111603

Liang, L. F., Xin, M. Y., and Wang, H. (2018). "Research of extraction of rice straw cellulose and feasibility of fiber formation," *Journal of Textile Science and Engineering* 35(3), 86-89. DOI: 10.3969/j.issn.2096-5184.2018.03.019

Liao, M., Sun, H., Zhang, J., Wu, J. X., Xie, S. L., Fu, X. M., Sun, X. M., Wang, B. J., and Peng, H. S. (2018). "Multicolor, fluorescent supercapacitor fiber," *Small* 14(43), Article ID 1702052. DOI: 10.1002/smll.201702052

Liu, W., Liu, S., Liu, T., Liu, T., Zhang, J., and Liu, H. (2019). "Eco-friendly post-consumer cotton waste recycling for regenerated cellulose fibers," *Carbohydrate Polymers* 206, 141-148. DOI: 10.1016/j.carbpol.2018.10.046

Lu, J. T. (2014). *The Preparation and Performance Study of Skin Repair Materials Based on Regenerated Cellulose*, Master's Thesis, Jiangnan University, Jiangsu, China.

Luzi, F., Fortunati, E., Jiménez, A., Puglia, D., Pezzolla, D., Gigliotti, G., Kenny, J. M., Chiralt, A., and Torre, L. (2016). "Production and characterization of PLA_PBS biodegradable blends reinforced with cellulose nanocrystals extracted from hemp fibres," *Industrial Crops and Products* 93, 276-289. DOI: 10.1016/j.indcrop.2016.01.045

Mahmoudian, S., Sazegar, M. R., Afshari, N., and Wahit, M. U. (2017). "Graphene reinforced regenerated cellulose nanocomposite fibers prepared by Lyocell process," *Polymer Composites* 38(S1), E81-E88. DOI: 10.1002/pc.23864

Ouyang, W. Z., Sun, J. H., Memon, J., Wang, C., Geng, J. X., and Huang, Y. (2013). "Scalable preparation of three-dimensional porous structures of reduced graphene oxide/cellulose composites and their application in supercapacitors," *Carbon* 62, 501-509. DOI: 10.1016/j.carbon.2013.06.049

Saba, N., Jawaid, M., Alothman, O. Y., and Paridah, M. T. (2016). "A review on dynamic mechanical properties of natural fibre reinforced polymer composites," *Construction and Building Materials* 106, 149-159. DOI: 10.1016/j.conbuildmat.2015.12.075

Sawangphruk, M., Srimuk, P., Chiochan, P., Krittayavathananon, A., Luanwuthi, S., and Limtrakul, J. (2013). "High-performance supercapacitor of manganese oxide/reduced graphene oxide nanocomposite coated on flexible carbon fiber paper," *Carbon* 60, 109-116. DOI: 10.1016/j.carbon.2013.03.062

Small, A. C., and Johnston, J. H. (2008). "Novel hybrid materials of cellulose fibres and doped ZnS nanocrystals," *Current Applied Physics* 8(3-4), 512-515. DOI: 10.1016/j.cap.2007.10.046

Tang, L. B., Ji, R. B., Li, X. M., Bai, G. X., Liu, C. P., Hao, J. H., Lin, J. Y., Jiang, H. X., Teng, K. S., Yang, Z. B., *et al.* (2014). "Deep ultraviolet to near-infrared emission and photoresponse in layered n-doped graphene quantum dots," *ACS Nano* 8(6), 6312-6320. DOI: 10.1021/nn501796r

Wang, J. J. (2014). *Preparation, Characterization and Nonlinear Optical Properties of Graphene-Carboxymethyl Cellulose Nano-composite Materials*, Master's Thesis, Fuzhou University, Fujian, China.

Wang, P., Tawiah, B., Tian, A., Wang, C., Zhang, L., and Fu, S. (2015). "Properties of alginate fiber spun-dyed with fluorescent pigment dispersion," *Carbohydrate Polymers* 118, 143-149. DOI: 10.1016/j.carbpol.2014.11.028

Wang, R. (2015). *Study on the Preparation and Properties of the Fluorescent Fibers*, Master's Thesis, Donghua University, Shanghai, China.

Yu, J. G., Yu, H. G., Cheng, B., Zhao, X. J., Yu, J. C., and Ho, W. K. (2003). "The effect of calcination temperature on the surface microstructure and photocatalytic activity of TiO2 thin films prepared by liquid phase deposition," *Journal of Physical Chemistry B* 107(50), 13871-13879. DOI: 10.1021/jp036158y

Zhang, H. H., Wang, R., Yang, G. S., Xu, Y. Y., and Shao, H. L. (2016). "UV-excitable fluorescent poly(lactic acid) fibers," *Polymer Engineering and Science* 56(4), 373-379. DOI: 10.1002/pen.24262

Zhang, H. R., Huang, S. P., Gong, J. H., Wu, J., and Xuan, Lu. (2003). "Property and structure of fluorescence fiber," *Shanghai Textile Science and Technology* 2, 13-15. DOI: 10.16549/j.cnki.issn.1001-2044.2003.02.004

Zhang, K., Zhang, L. L., Zhao, X. S., and Wu, J. S. (2010). "Graphene/polyaniline nanofiber composites as supercapacitor electrodes," *Chemistry of Materials* 22(4), 1392-1401. DOI: 10.1021/cm902876u

Zhang, Y. C., Jiang, Y., Han, L., Wang, B., Xu, H., Zhong, Y., Zhang, L., Mao, Z., and Sui, X. (2018). "Biodegradable regenerated cellulose-dispersed composites with improved properties *via* a pickering emulsion process," *Carbohydrate Polymers* 179, 86-92. DOI: 10.1016/j.carbpol.2017.09.065

Zhang, Y. Y., and Cheng, Q. F. (2019). "Progress in research of graphene nanocomposite fibers," *Materials China* 38(1), 49-57. DOI: 10.7502/j.issn.1674-3962.2019.01.06

Zhao, C. X., Gao, X. N., and Feng, L. Q. (2012). "Application of luminescent fiber on knitted fabric," *Jiangsu Silk* 5, 35-38.

Zhao, L. Y., Zhang, R. Y., Deng, C. Y., Peng, Y. X., and Jiang, T. (2019). "Tunable infrared emissivity in multilayer graphene by ionic liquid intercalation," *Nanomaterials* 9(8), Article number 1096. DOI: 10.3390/nano9081096

Article submitted: January 17, 2020; Peer review completed: April 3, 2020; Revised version received and accepted: April 20, 2020; Published: April 27, 2020.
DOI: 10.15376/biores.15.2.4434-4448